

INVESTIGATING THE ROLE OF IRON SULFUR CLUSTER
BINDING RESIDUES OF HYDF

by

Neelambari Joshi

A thesis submitted in partial fulfillment
of the requirements for the degree

of

Master of Science

in

Biochemistry

MONTANA STATE UNIVERSITY
Bozeman, Montana

April 2012

©COPYRIGHT

by

Neelambari Joshi

2012

All Rights Reserved

APPROVAL

of a thesis submitted by

Neelambari Joshi

This thesis has been read by each member of the thesis committee and has been found to be satisfactory regarding content, English usage, format, citation, bibliographic style, and consistency and is ready for submission to The Graduate School.

Dr. John W. Peters

Approved for the Department of Chemistry and Biochemistry

Dr. Bern Kohler

Approved for The Graduate School

Dr. Carl A. Fox

STATEMENT OF PERMISSION TO USE

In presenting this thesis in partial fulfillment of the requirements for a master's degree at Montana State University, I agree that the Library shall make it available to borrowers under rules of the Library.

If I have indicated my intention to copyright this thesis by including a copyright notice page, copying is allowable only for scholarly purposes, consistent with "fair use" as prescribed in the U.S. Copyright Law. Requests for permission for extended quotation from or reproduction of this thesis in whole or in parts may be granted only by the copyright holder.

Neelambari Joshi

April 2012

ACKNOWLEDGEMENTS

I would like to express my sincere gratitude to Dr. John W. Peters for his detailed continuous support and motivation in my master's studies. Under his guidance I learned a lot about research.

I am deeply grateful to my committee members Dr. Joan Broderick and Dr. Brian Bothner for providing guidance as well as critical insights regarding my project.

I owe a note of gratitude to Dr. Eric M. Shepard for his untiring assistance, detailed discussions regarding my work.

I would like to thank, Dr. Trinity Hamilton, Jesse Therien, Kevin Swanson for their essential contributions and constructive criticism regarding my work.

Many thanks to the lab members Dr. Danillo Ortillo, Dr. Oleg Zadvornyy, Dr Eric Boyd, Matthew Urschel, Steve Keable, Cate Burgess, Alta Howells for their help.

I owe my sincere thanks to Mr. Shourjo Ghose for his academic as well as moral support. Last but not the least I want to thank my family for believing in me.

My work was supported by the NASA Astrobiology Institute, Montana State University, Astrobiology Biogeocatalysis Research Center.

TABLE OF CONTENTS

1. INTRODUCTION	1
Iron Sulfur Clusters in Biology	1
[FeFe]-Hydrogenases	2
[FeFe]-Hydrogenases Maturation	3
Maturation Enzymes HydE and HydG	5
Maturation Enzyme HydF.....	7
2. MATERIAL AND METHODS	14
Site Directed Mutagenesis of HydF from <i>Clostridium acetobutylicum</i>	14
Cell Growth.....	15
Protein Purification	16
Quantifying Protein and Iron Content.....	17
EPR Sample Preparation and Spectroscopic Analysis.....	18
<i>In vitro</i> Hydrogenase Activity Assays	19
3. DATA AND RESULTS	21
Iron Content of HydF ^{ΔEG} Mutants	21
UV-Vis Absorption spectroscopy of HydF ^{ΔEG} Mutants	22
EPR Spectroscopy	27
C353S HydF ^{ΔEG}	27
H306Q HydF ^{ΔEG}	28
<i>In vitro</i> Hydrogenase Activity Assays	31
4. DISCUSSION.....	33
REFERENCES CITED.....	37

LIST OF TABLES

Table	Page
1. Mutagenic oligonucleotides	15
2. Iron assay for WT and mutant HydF ^{ΔEG}	22

LIST OF FIGURES

Figure	Page
1. Examples of simple iron-sulfur clusters in biology containing one, two, three and four iron atoms (coloring scheme: iron:rust, sulfur:yellow, oxygen:red, carbon:gray, nitrogen:blue).....	1
2. A) The di-metallic active site of the [NiFe]-hydrogenase (iron rust, nickel green, sulfur yellow, nitrogen blue, oxygen small red) B) The H-cluster active site of the [FeFe]- hydrogenase (colors same as Fig.1, with unknown dithiolate atom pink).....	2
3. Model for activation of HydA ^{ΔEFG} . Accessory protein complex containing HydE, HydF and HydG acts in concert to synthesize an H-cluster precursor (*), which is transferred to the structural enzyme resulting in activation of [FeFe]-hydrogenase.....	4
4. Mechanism of cleavage of S-adenosylmethionine by a [4Fe-4S] ⁺ cluster, forming methionine and a 5''-deoxyadenosyl radical.....	6
5. HydG catalyzes the synthesis of CO and CN ⁻ using tyrosine as a substrate.....	7
6. Detailed illustration of the region of the tetramer around putative FeS cluster binding sites. Cartoons of monomers belonging to two different dimers are shown in green and cyan, respectively. Side chains of Cys 302, 353 and 356 and His 304 and 352 are shown as ball-and-stick representation (red and yellow for monomers A and D, respectively). Cys 302 of monomers belonging to two different dimers form an intermolecular disulfide bridge; whereas, Cys 353 and 356 form an intramolecular disulfide bond within respective monomers.....	11
7. Amino acid sequence of <i>C.acetobutylicum</i> (CLOACE) aligned with <i>S.oneidensis</i> (SHEWONE), <i>T.neapolitana</i> (THENN), <i>T.maritima</i> (THEMA). Red block represents consensus C-terminal Fe-S cluster binding residues (CxHx ₄₅₋₅₃ CxxC).....	13
8a. UV-Vis absorption spectra of WT, C304S and C304A HydF ^{ΔEG} <i>C.acetobutylicum</i> (50μM each). The optical pathlength was 1cm.....	23

LIST OF FIGURES CONTINUED

Figure	Page
8b. UV-Vis absorption spectra of WT, H306Q, H306N and H306A HydF ^{ΔEG} <i>C.acetobutylicum</i> (50μM each). The optical pathlength was 1cm.....	24
8c. UV-Vis absorption spectra of WT, C353S and C353A HydF ^{ΔEG} <i>C.acetobutylicum</i> (50μM each). The optical pathlength was 1cm.....	25
8d. UV-Vis absorption spectra of WT, C356S and C356A HydF ^{ΔEG} <i>C.acetobutylicum</i> (50μM each). The optical pathlength was 1cm.....	26
9a. Low temperature EPR signal of as-isolated C353S HydF ^{ΔEG} (g= 2.04, 2.01,1.97).....	27
9b. Low temperature EPR signal of reduced C353S HydF ^{ΔEG} shows presence of a [4Fe4S] ⁺ (g _⊥ = 1.89 and g _∥ = 2.05) C353S HydF ^{EG} - Black line- w/o GTP Red line- with GTP	28
10a. Low temperature EPR signal of as-isolated H306Q HydF ^{ΔEG} shows presence of a [4Fe-4S] ⁺ (g _⊥ = 1.895 and g _∥ = 2.05) and [2Fe-2S] ⁺ cluster (g= 2.00, 1.96).....	29
10b. Low temperature EPR signal of reduced H306Q HydF ^{ΔEG} shows presence of a [4Fe4S] ⁺ (g _⊥ = 1.89 and g _∥ = 2.05) . H306Q HydF ^{EG} - Black line- w/o GTP Red line- with GTP.....	30
10c. Temperature dependence of as-isolated sample of HydF ^{ΔEG} H306Q in the presence of MgCl ₂ (5 mM). EPR parameters are given in experimental procedures. Samples were run at a constant power setting (1.85 mW) at the temperature values given for each spectrum.....	30
11. H ₂ evolution assays to probe the effects of HydF mutations on the activation of HydA ^{ΔEFG} by HydF ^{EG}	33

LIST OF FIGURES CONTINUED

Figure	Page
12. Proposed models (A and B) for putative ligations of the [4Fe-4S] and the [2Fe-2S] clusters to the polypeptide chain as inferred from the site directed mutagenesis experiments.....	36

ABSTRACT

[FeFe]-hydrogenases are metalloenzymes found in many bacteria and lower eukaryotes. The catalytic active site of [FeFe]-hydrogenases termed as H-cluster consists of a [4Fe-4S] cubane bridged to a 2Fe subcluster. The two iron atoms of the 2Fe subcluster are decorated by carbon monoxide, cyanide ligands as well as a bridging dithiolate ligand. The assembly of this complex H cluster involves the role of three accessory enzymes namely HydE, HydG and HydF. The maturase, HydF is a GTPase and contains two types of clusters, a [4Fe-4S] and a [2Fe-2S] cluster. The [2Fe-2S] cluster is transformed into an H-cluster precursor by action of HydE and HydG. It is suggested from EPR spectroscopic data of both reduced HydF^{ΔEG} and Oxidized HydF^{EG} that the [2Fe-2S] cluster and the [4Fe-4S] cluster are not bound to each other. Since an H-cluster like signal was observed in oxidized HydF^{EG} suggested that the two clusters are arranged in same manner as the H-cluster itself. This aforementioned hypothesis drove us to investigate the ligand arrangement of both a [4Fe-4S] and most importantly the [2Fe-2S] clusters in HydF. The apo HydF structure does not provide us with significant insights into Fe-S cluster coordination details, therefore we have attempted to experimentally identify the residues that act as ligands to both the clusters. To that end, we substituted each of the conserved Fe-S cluster binding residues and observed the effects of these mutations on both clusters by spectroscopic methods like UV-Vis spectroscopy and EPR. Our observations indicated that among the three conserved cysteines, C304 and C356 are absolutely quintessential for iron sulfur cluster assembly in HydF^{ΔEG} while C353 and H306 have some capacity to bind iron sulfur clusters. Further *in vitro* hydrogenase assays suggested importance of C353 residue as it affected the assembly of the 2Fe subcluster. Thus we propose a dimeric/ tetrameric model of HydF where both the [2Fe-2S] and the [4Fe-4S] clusters are ligated by eight conserved, four putative Fe-S cluster binding residues from each monomer. In our proposed model we discuss the possible occurrence of non cysteinyl ligation for iron sulfur clusters.

INTRODUCTION:

Iron Sulfur Clusters in Biology

Iron sulfur clusters have been implicated to serve in a variety of roles including electron transport, biosynthesis of enzymes, regulation of gene expression and iron storage. These clusters have also been shown to play essential roles in many biologically important reactions like nitrogen fixation, oxidative phosphorylation, and photosynthesis (1-3). Iron sulfur clusters are known to be ligated by a variety of ligands such as cysteine, arginine and histidine. This coordination environment directly affects the redox potential of these clusters which can range from -0.6 V to 0.45 V (4, 5). The most common type of iron sulfur clusters having diversity in function and reactivity are single Fe, [2Fe-2S], [3Fe-4S] and [4Fe-4S] (Fig.1). Sometimes iron sulfur clusters are structurally modified to broaden their range of chemical reactivities and functions, as seen in enzymes like nitrogenase, acetyl coA synthase, as well as hydrogenases such as [NiFe]- and [FeFe]-hydrogenases (4).

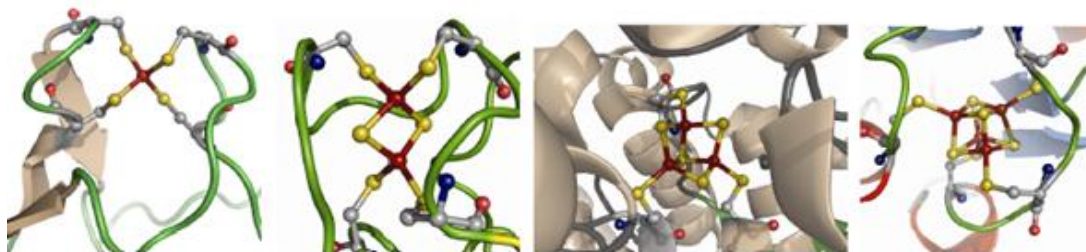


Fig.1. Examples of simple iron-sulfur clusters in biology containing one, two, three and four iron atoms (coloring scheme: iron:rust, sulfur:yellow, oxygen:red, carbon:gray, nitrogen:blue) (4)

[FeFe]-Hydrogenases

Among several [Fe-S] cluster containing proteins, the two classes of hydrogenases, the [NiFe]- and the [FeFe]- hydrogenases are known to catalyze reversible oxidation of hydrogen and proton reduction ($\text{H}_2 \leftrightarrow 2\text{H}^+ + 2\text{e}^-$) (6-10). Hydrogenases either function to dispose off excess electrons accumulated during bacterial fermentation or couple hydrogen oxidation to energy yielding processes (11). The [NiFe]- and [FeFe]- hydrogenases differ both phylogenetically (11) and in metal content at the active site. The [NiFe]- hydrogenases active site contain an iron atom ligated to one carbon monoxide and two cyanide ligands and bridged to a nickel atom via two cysteine thiolate ligands (12) (Fig.2A).

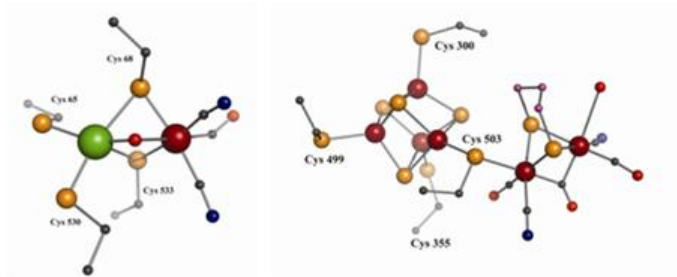


Fig.2. A) The di-metallic active site of the [NiFe]-hydrogenase (iron rust, nickel green, sulfur yellow, nitrogen blue, oxygen small red) B) The H-cluster active site of the [FeFe]- hydrogenase (colors same as above, with unknown dithiolate atom pink) (12, 13)

The [FeFe]-hydrogenase active site contains a [4Fe-4S] cluster linked by a cysteinyl thiolate to a [2Fe] subcluster coordinated by carbon monoxide and cyanide ligands (Fig.2B) (13). In addition to these ligands, the Fe ions of the [2Fe] subcluster are bridged by a non-protein dithiolate linkage which is proposed to be propane dithiolate (14), dithiomethyl amine (15) or dithiomethyl ether (16). Recent ^{14}N HYSCORE

investigation of the H-cluster of [FeFe]-hydrogenase by Lubitz et al suggested the presence of nitrogen in the dithiolate linkage assigning it as a dithiomethyl amine ligand. It is further suggested that the NH group at the bridge head can act as a catalytic base during reactions (17).

The mechanism for the assembly of complex protein based metalloclusters has intrigued biochemists for decades. To that end, the biosynthesis of the H-cluster in [FeFe]-hydrogenases is no different. The mutant studies on the green algae *Chlamydomonas reinhardtii* (*C. r.*) have revealed that the gene products namely HydEF and HydG are essential in the assembly of active [FeFe]-hydrogenase and for hydrogen production. Thus the action of three genes *hydE*, *hydG* and *hydF* is shown to be absolute requirement for [FeFe]-hydrogenase maturation (18). Further it was observed that HydE, HydG and HydF from *Clostridium acetobutylicum* (*C. a.*) and HydA from *Clostridium acetobutylicum* (*C. a.*), *Clostridium pasteurianum* (*C. p.*) and *Chlamydomonas reinhardtii* (*C. r.*) when co-expressed in *Escherichia coli* (*E. coli*) facilitated formation of active [FeFe]-hydrogenases (20). These genes, *HydE*, *HydG* and *HydF* have been found to be in the genomes of all organisms in which active [FeFe]-hydrogenases are found (18).

[FeFe]-Hydrogenase Maturation

Discovery of these three accessory proteins (HydE, HydF and HydG) directed us to propose a hypothesis for the assembly of the H-cluster active site. This hypothesis includes a possible mechanism for the action of these maturation proteins which leads to biosynthesis of the precursor, containing the CN⁻ and CO and the dithiolate ligands. The

insertion of this precursor in the H-cluster then results in activation of the [FeFe]-hydrogenase (27).

To investigate the action of maturation proteins on [FeFe]-hydrogenase, an *in vitro* *E. coli* based system was developed in which [FeFe]-hydrogenase structural protein, also known as HydA was expressed in the absence of the accessory proteins (HydA^{ΔEFG}). Surprisingly it was observed that HydA^{ΔEFG} can exist as a stable protein but does not exhibit any hydrogenase activity (the hydrogenase activity is determined by hydrogen production assay). This inactive HydA^{ΔEFG} was observed to get activated by the addition of the cellular extracts in which the three accessory proteins, HydE, HydF and HydG from *Clostridium acetobutylicum* were co-expressed without HydA. The production of measurable amounts of H₂ was then correlated to the activation of HydA^{ΔEFG} (21) (Fig.3).

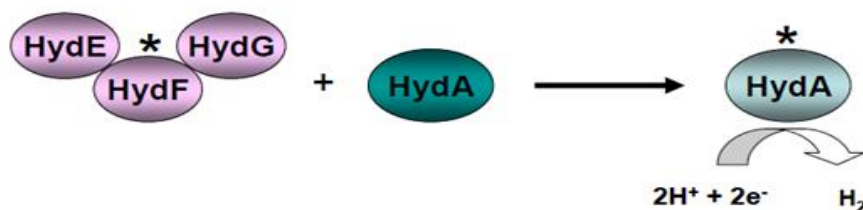


Fig.3. Model for activation of HydA^{ΔEFG}. Accessory protein complex containing HydE, HydF and HydG acts in concert to synthesize an H-cluster precursor (*), which is transferred to the structural enzyme resulting in activation of [FeFe]-hydrogenase (21).

The ability to form activated HydA upon addition of cellular extracts containing HydE, HydG and HydF together, resulted in the hypothesis that a specific interaction must occur between HydA and at least one of the accessory proteins resulting in hydrogenase maturation. It was proposed that either HydE or HydG, being members of

the radical SAM super family were involved in the synthesis of the CO, CN⁻ as well as the bridging dithiolate ligands from the common metabolite or amino acid within the cell. Furthermore, it was suggested that one of the accessory enzymes, probably HydF act as metal cluster carrying scaffold that delivers the precursor required for HydA activation. Therefore, to determine the role of the accessory proteins in HydA activation, suitable genetic constructs were made using HydE, HydF and HydG from *C. acetobutylicum*. These constitute, HydE co-expressed with HydF and HydG (HydE^{FG}), HydG co-expressed with HydF and HydE (HydG^{EF}), HydF co-expressed with HydE and HydG (HydF^{EG}) etc (28). Among all these constructs only HydF co-expressed with HydE and HydG (HydF^{EG}) was able to activate HydA^{ΔEFG} (28). The above experiments indicated that HydF^{EG} has the ability to activate HydA^{ΔEFG} but when HydF is expressed singly, in the absence of HydE and HydG (HydF^{ΔEG}) its activating ability is lost. These results identify the role of HydE and HydG in the precursor assembly process with a scaffold/carrier HydF (28).

Maturation Enzymes HydE and HydG

Radical S- adenosyl methionine (radical SAM) enzymes are characterized by conserved C_{x3}C_{x2}C motif which binds a redox active site-differentiated [4Fe-4S] cluster that coordinates SAM at the unique iron (18, 33). The SAM undergoes reductive cleavage resulting in a 5'-deoxyadenosyl radical and methionine (Fig.4) with the resulting radical then abstracting a hydrogen atom from the substrate. This substrate radical is then involved in a variety of radical based chemistry (34). Radical SAM enzymes catalyze a

variety of reactions, including the formation of glycol radicals, isomerization reactions, and sulfur insertions (19).

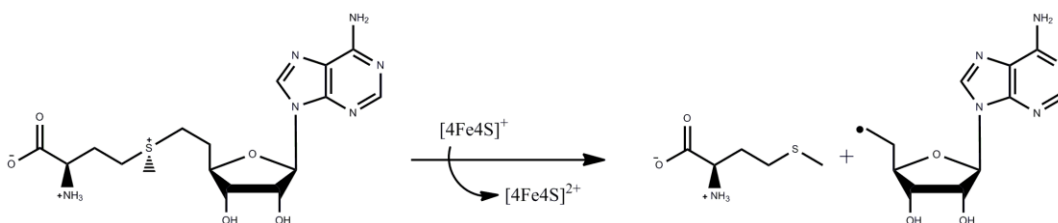


Fig.4. Mechanism of cleavage of S-adenosylmethionine by a $[4\text{Fe-4S}]^+$ cluster, forming methionine and a 5'-deoxyadenosyl radical (19).

Initial biochemical studies of HydE and HydG have demonstrated that they both show characteristic features of radical SAM enzymes including the ability to cleave SAM and to bind iron sulfur clusters (23). The mutations in the conserved radical SAM cluster binding motif in HydG from *Clostridium acetobutylicum* resulted in significant loss of hydrogenase activity in whole cell extracts suggested its importance in H-cluster assembly (20). HydG shares significant sequence similarity with another radical SAM enzyme ThiH, tyrosin lyase (25) and recently it has been shown that HydG in the presence of SAM was able to cleave tyrosine resulting in the formation of CO and CN- ligands (35, 36) (Fig.5).



Fig.5. HydG catalyzes the synthesis of CO and CN⁻ using tyrosine as a substrate

The crystal structure of reconstituted HydE from *Thermotoga maritima* revealed the presence of a site differentiated [4Fe-4S] cluster with SAM bound along with a [2Fe-2S] cluster confirming that it had a complete TIM (triose-phosphate isomerase) type $\alpha_8\beta_8$ barrel structure (26). It was also suggested that mutations in the conserved radical SAM cluster binding motif in HydE from *Clostridium acetobutylicum* resulted in the loss of hydrogenase activity in whole cell extracts suggesting essential role for radical SAM chemistry in maturation of hydrogenase (20). HydE shares sequence and structural similarity with another radical SAM enzyme, Biotin synthase (BioB) (24). BioB catalyses sulfur insertion reaction into dethiobiotin to form biotin (24). A specific substrate on which HydE has not been identified yet but it is proposed to carry out the sulfur insertion reaction required for the synthesis of the bridging dithiolate ligand of the H-cluster.

Maturation Enzyme HydF

Another maturase protein required for [FeFe]-hydrogenases maturation is HydF. The amino acid sequence alignment along with the apo, GTP free tetrameric (dimer of dimers) structure of HydF from *T.neapolitana* suggests that HydF is composed of three domains. Domain I or N-terminal domain contains a GTP binding pocket while domain II

is responsible for HydF dimerization and lastly domain III or C-terminal domain contains putative Fe-S cluster binding residues (20, 48).

The N-terminus of HydF has a Walker A P loop which binds the phosphate groups of the GTP and a Walker B Mg^{2+} binding loop (20). The GTPase activity of HydF from *C. acetobutylicum* has shown higher turnover rate than the *T. maritima* enzyme (22, 30). It was also demonstrated that GTPase activity of HydF from *C. acetobutylicum* is dependent on monovalent cation size, showing greatest activity in the presence of K^+ which is comparable to other GTPase (30). Interestingly it was observed that GTPase activity is independent of the iron sulfur cluster content of HydF. It has also been shown that mutations in the Walker P-loop results in inactive hydrogenase. To that end our lab carried out hydrogenase activity assays in the presence of GTP, GDP and non-hydrolysable GTP analogs but was unable to detect any facilitation in precursor delivery by HydF^{EG} to HydA^{ΔEFG} upon GTP addition (20). Although GTP hydrolysis was shown to be non essential in the final step of H-cluster maturation, it was however observed that the rate HydF catalyzed GTP hydrolysis rate was increased by ~50% in presence of HydE and HydG. This indicates that GTP hydrolysis could be utilized elsewhere in the precursor assembly and not in final precursor delivery step (30).

The C-terminal domain of HydF contains the conserved amino acid sequence (CxHx₄₆₋₅₃CxxC) comprising the putative ligands for the iron sulfur cluster (20). The initial spectroscopic characterization of reconstituted reduced HydF^{ΔEG} from *T. maritima* showed spectral features indicative of a $[4Fe-4S]^+$ cluster with a ligand exchangeable site (22). Subsequent temperature dependent EPR studies of the non reconstituted reduced HydF^{ΔEG} from *C. acetobutylicum* displayed signals for 2 types of iron sulfur clusters, a

[2Fe-2S]⁺ and a [4Fe-4S]⁺ (30). Intriguingly, the signal for [2Fe-2S]⁺ cluster is not detected in the non reconstituted reduced HydF^{EG} suggesting [2Fe-2S] cluster became diamagnetic. Further these results were linked to a possible interactive role between HydF with HydE and HydG (30). The EPR spectral intensities of Fe-S clusters on both HydF^{ΔEG} and HydF^{EG} were increased on the addition of GTP indicated a direct communication between the Fe-S cluster binding domain and the GTPase domain. Previous work had established that HydF^{EG} has the capacity to activate HydA^{ΔEFG}, therefore to understand nature of the modified species on HydF^{EG}, our group performed FTIR experiments on heterologously expressed HydF from *C. acetobutylicum*. Our results indicated that HydF^{EG} produced spectra indicative of a Fe atom ligated to CO and CN⁻ species. These results were similar to what has been observed in homologously expressed HydF^{EG} and in the H-cluster of active [FeFe]-hydrogenase (30). Further, X-ray crystallographic and spectroscopic studies demonstrated that HydA^{ΔEFG} contains an [4Fe-4S] cluster assembled by the cell's innate Fe-S cluster assembly mechanism (32, 43). Therefore it was suggested that the 2Fe subcluster is built on and delivered by HydF^{EG} to produce active hydrogenase.

The X-ray crystal structure of apo, GTP free form of HydF from *Thermotoga neapolitana* (*T. n.*) was recently published (48). The asymmetric unit in the tetrameric (dimer of dimers) structure is a monomer. The monomer contains three domains, GTP binding domain or domain I, domain II which is responsible for HydF dimerization and domain III or the Fe-S cluster binding domain. HydF dimerization is invoked through domain II. The dimeric form of HydF seems a solvent accessible form that can interact with its potential partners. The tetramer which is formed by dimerization of dimers is a

closed conformation where the Fe-S cluster binding site is inaccessible. Although no Fe-S cluster was bound in the tetrameric (dimer of dimers) structure of HydF a Fe-S cluster binding pocket made with 3 conserved cysteines and a conserved histidine and a not absolutely conserved histidine was detected (Fig.6, 48). Subsequently mutations in two of the conserved cysteines (C353 and C356) in HydF from *C. acetobutylicum* resulted in inactive hydrogenase which confirmed their importance but the specific reason is still unknown. HYSCORE studies performed on HydF^{EG} from *C. acetobutylicum* indicated the presence of a histidine nitrogen ligation in [4Fe-4S] cluster as it was observed in reconstituted *T.maritima* HydF^{ΔEG} (22, 41). However, Czech et al observed an H-cluster like signal from the oxidized HydF^{EG} and proposed a model for Fe-S cluster in HydF similar to the H-cluster itself where two of the cysteines and a histidine residue binds a [4Fe-4S] cluster while the third cysteine residue act as a bridging ligand between a [4Fe-4S] and the 2Fe species (42). Currently there are only speculations regarding the arrangement of a [4Fe-4S] cluster and the 2Fe subcluster in HydF without a real understanding of the residues that are essential for ligation of the said clusters. It is observed that in proteins cysteines are the most commonly observed ligands for iron coordination in the [Fe-S] clusters; however other residues like histidine have also been shown to participate in the cluster ligation (5).

The amino acid sequence alignment (Fig.7) from four different microbial sources *C.acetobutylicum* (CLOACE), *S.oneidensis* (SHEWONE), *T.neapolitana* (THENN) and *T.maritima* (THEMA) show presence of a putative Fe-S cluster binding residues (CxHx₄₅₋₅₃CxxC) which contain three conserved cysteines and one histidine. Thus we decided to employ site directed mutagenesis to substitute each of the conserved Fe-S cluster

binding amino acid residues and analyze the effects of these changes in protein coordination on

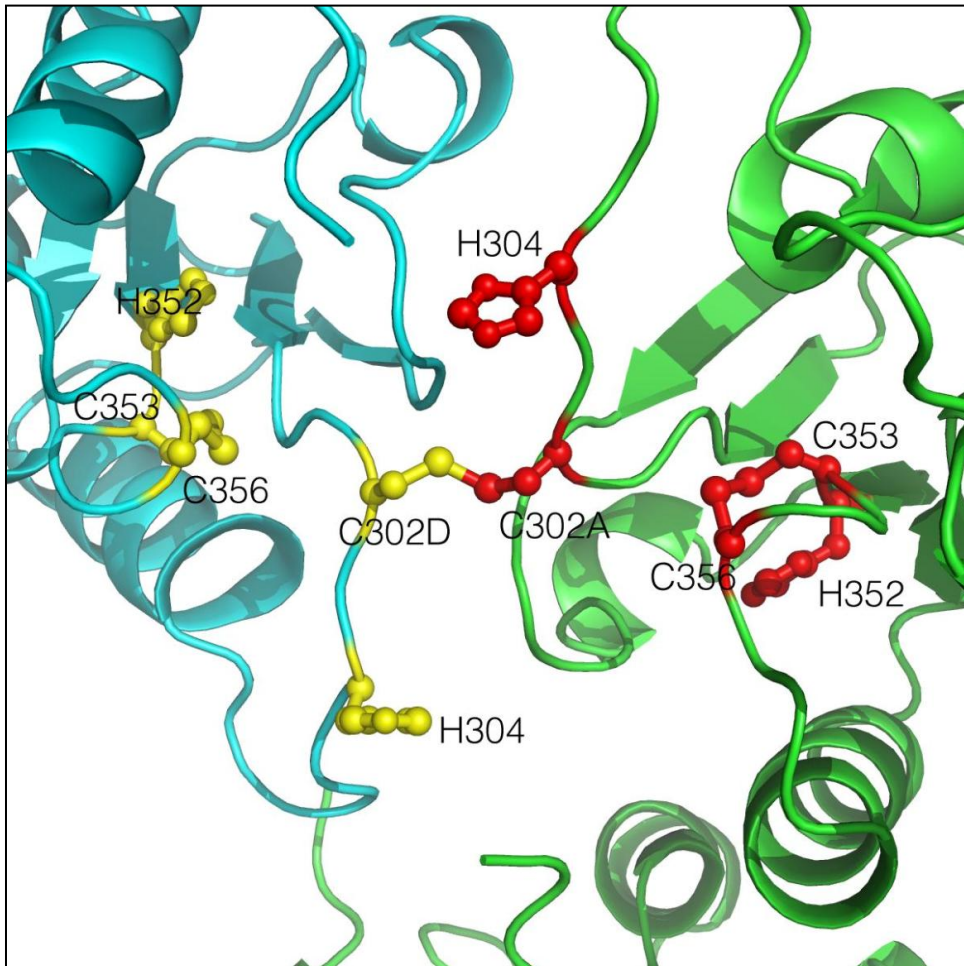


Fig.6: Detailed illustration of the region around putative Fe-S cluster binding sites in the dimer of dimer (tetramer) structure of HydF from *T. neapolitana*. Cartoons of monomers belonging to two different dimers are shown in green and cyan, respectively. Cys 302 of monomers belonging to two different dimers form an intermolecular disulfide bridge; whereas, Cys 353 and 356 form an intramolecular disulfide bond within respective monomers (48).

both [4Fe-4S] and [2Fe-2S] clusters. HydF from *C. acetobutylicum* (C_xH_x₄₅C_{xx}C) was used and substituted to following residues: C304S/A, C353S/A, C356S/A, H306Q/N/A.

Our preference for the substitution of residues was dictated in a way such that the substituted residue may undergo loss of interaction with the cluster or it may interact with the cluster in a novel way (modified interactions from the alternative side chain). The substitution of deprotonated cysteine to deprotonated serine replaces a sulfur atom with oxygen which is proposed to cause a small change in the coordination environment of the cluster, while alanine is a suitable replacement for both cysteine and histidine as it has a shorter side chain and has no atoms that could potentially bind Fe in the Fe-S clusters.

Histidine contains the imidazol $\epsilon 2$ and $\delta 1$ nitrogen atoms and deprotonated nitrogen atoms can coordinate with Fe ions using a lone pair on either nitrogen atoms. Since it is unknown that which nitrogen could act as ligand for Fe-S cluster in HydF, we decided to substitute histidine to glutamine (ϵ amide oxygen) and asparagine (δ amide oxygen), respectively.

We have employed a variety of tools such as biochemical assays as well as spectroscopic methods such as Electron Paramagnetic Resonance and UV-vis Spectroscopy to probe the effects of the ligand mutations on HydF.

MATERIAL AND METHODS

Site Directed Mutagenesis of HydF from *Clostridium acetobutylicum*

The single or multiple base substitutions in *hydF* were constructed via a site directed mutagenesis kit by Promega. Wild type HydF (*C.acetobutylicum*) in pRSFDUET-1 plasmid (Promega) was used for all DNA manipulations. Primers were designed and ordered from Integrated DNA Technologies (USA) to get the substituted genes by polymerase chain reaction (PCR) (Table.1.). The plasmids containing the gene were then run on an 8% agarose gel to confirm the correct size plasmid. The substituted gene containing plasmids were then transformed into *E.coli* JM-109 (Promega) cells for propagation and subsequently purified using a Promega spin miniprep kit. The plasmid DNA was then sent for sequencing to Arizona State Genomic Centre to confirm their fidelity. The plasmids with the correct mutations were then transformed into *E. coli* BL21 (DE3) cells (Stratagene) for protein expression.

Table:1 Mutagenic Oligonucleotides
C304SFWD: 5'- GCAGAAGCCAGCACCCACCACCGTCAATCTGATGATATAGGT -3'
C304S REV: 5'- ACGGTGGTGGGTGCTGGCTTCTGCTATTTAAAAT -3'
C304AFWD: 5'- GCAGAAGCCGCAACCCACCACCGTCAATCTGATGATATAGGTAAAGTA-3'
C304AREV:5'-ATCATCAGATTGACGGTGGTGGGTTGCGGCTTCTGCTATTTAAAATTTTATC-3'
H306QFWD: 5'- GAAGCCTGCACCCAGCACCGTCAATCT -3'
H306Q REV: 5'- AGATTGACGGTGGTGGTGCAGGCTTC -3'
H306N FWD: 5'- GCAGAAGCCTGCACCAATCACCGTCAATCTGATGATATAGGT -3'
H306N REV: 5'- ATCAGATTGACGGTGGTGGTGCAGGCTTCTGCTATTTAAAATTTTATC -3'
H306A FWD: 5'- GCAGAAGCCTGCACCCGACACCGTCAATCTGATGATATAGGT -3'
H306AREV:5'- ATCAGATTGACGGTGGTGGTGCAGGCTTCTGCTAT TAAAATTTTATC -3'
C353S FWD: 5'- GCACTTATAGTTCATGCAGCTGGCTGCATGCTAAACAGA -3'
C353S REV: 5'- TCTGTTTAGCATGCAGCCAGCTGCATGAACTATAAGTGC -3'
C353A FWD: 5'- GCACTTATAGTTCATGCAGCTGGCTGCATGCTAAACAGA -3'
C353A REV: 5'- CATGCAGCCAGCCGCATGAACTATAAGTGCATAATCCTC -3'
C356S FWD: 5'- GCTGGCAGCATGCTAAACAGACGTTCA -3'
C356S REV: 5'- GTTTAGCATGCTGCCAGCACAATGAAC -3'
C356A FWD: 5'- GTTCATTGTGCTGGCGCAATGCTAAACAGACGTTCAATG -3'
C356A REV: 5'- TCTGTTTAGCATTGCGCCAGCACAATGAACTATAAGTGC -3'

Cell Growth

Genetic constructs encoding HydF substituted genes from *C. acetobutylicum* were transformed into *E. coli*- BL21 (DE3) (Stratagene) cells for protein expression (28). For substitutions of HydF^{ΔEF} Lauria Bertani broth (LB) agar plates with 30μg/mL kanamycin

were used while for altered HydF^{EG} LB agar plates with 50µg/mL ampicillin, 30µg/mL kanamycin, and 50µg/mL streptomycin were used. Single colonies obtained from these transformations were grown overnight in 50ml of LB media containing appropriate antibiotics at a 37°C incubator shaker at 250rpm. The overnight growth (e.g. ten 5 mL aliquots) was then transferred to 10 1L flasks of phosphate buffered LB pH 7.5 (including appropriate antibiotics), supplemented with 5.5g/L glucose and grown with shaking at 250 rpm to an optical density of 0.5-0.6 at 600 nm. Once the desired OD was reached the cells were induced with IPTG (Isopropyl β-D-1-thiogalactopyranoside) (1mM final concentration) and supplemented with 0.075 g/L ferrous ammonium sulfate. Cells were allowed to grow with shaking for an additional 2 hours, then they were allowed to cool on the bench top for 15 minutes before being purged with nitrogen at 4°C overnight. The cells were then centrifuged at 8,000 rpm for 10 minutes at 4°C. The supernatant was decanted and the cell pellets were frozen in liquid N₂ and stored at -80°C.

Protein Purification

All purification procedures were carried out under strictly anaerobic conditions in a Coy chamber unless otherwise noted. Cells were mixed with five volumes (e.g. 50 mL per 10g cells) of lysis buffer, composed of Buffer A (50mM HEPES, 0.5M KCl, 5% glycerol, 10 mM imidazole, pH 7.4), 1% Triton X-100, 5 µM PMSF, 9 mg/50mL lysozyme, trace amounts of RNase A and DNase I. The lysis was carried out over the course of 90 minutes by repetitively passing the suspension through a syringe. The suspension containing the lysed cells were then, put in centrifuge tubes and were sealed with screw caps containing O-rings so as to keep the contents anaerobic. The capped

centrifuge tubes were removed from the anaerobic chamber and centrifuged at 4°C at 18,000 rpm for 30 minutes. The tubes were returned to the Coy chamber and the supernatant was loaded onto a HisTrap™ HP Ni²⁺ affinity column (GE healthcare) previously equilibrated with 10 column volumes Buffer A. Buffer A was utilized for column equilibration and washing. The protein elution was accomplished by increasing the imidazole concentration in a stepwise manner from 20% to 50% to 100% using buffer B (50 mM HEPES buffer, pH 7.5, 0.3 M NaCl, 10% glycerol, 500 mM imidazole). The protein was further concentrated using an Amicon concentrator fitted with an YM-10 membrane. Then the protein was run over pre-equilibrated desalting G-25 column (GE healthcare) with Buffer A. After desalting it was flash frozen in liquid N₂ and stored at –80°C or in liquid N₂ until further use. The concentration of the protein was determined by Bradford assay (31). The purity of the protein sample was ascertained by separation through sodium dodecyl sulfate polyacrylamide gel electrophoresis (SDS PAGE). The separated protein was then visualized by staining the gel with coomassie brilliant blue followed by a prolonged period of de-staining in methanol and acetic acid.

Quantifying Protein and Iron Content

Protein concentration was determined by Bradford assay (31) with bovine serum albumin (BSA) as a standard. Seven standards were prepared, ranging in concentration from 0 to 6 µg/mL BSA. A 1:100 dilution of the unknown protein sample was made, then 3 to 6 samples were prepared with further dilution of the protein sample, typically ranging from 10 to 60 µL sample into 0.8 mL final volume prior to the addition of Bradford dye. The addition of Bradford Dye (200 µL) resulted in the final sample volume

to 1 mL. The samples were then incubated at room temperature for 60 minutes, and the absorbance was measured at 595 nm.

Iron content was determined by an iron assay (37). Six 1 mL dilutions of a Fe standard ranging from 0 to 2 $\mu\text{g}/\text{mL}$ were prepared. Protein samples (200 μL) were diluted to 1 mL with water, then two 3-fold and two 6-fold dilutions were made with a final sample volume of 1 mL for each dilution. Once dilutions were prepared, 500 μL Reagent A (1:1 1.2M HCl, 4.5% KMnO_4) was added to each sample, and all samples were gently vortexed and incubated in a 65°C water bath for 2 hours. After 2 hours, 100 μL Reagent B (5M ammonium acetate, 2 M ascorbic acid, 15 mM neocuprine, 6 mM ferrozine) was added, and samples and standards were incubated at room temperature for 30 minutes. The absorbance was then read at 562 nm (with reference wavelength at 900 nm).

EPR Sample Preparation and Spectroscopic Analysis

Electron paramagnetic resonance (EPR) samples of H306Q and C353S HydF^{ΔEG} were prepared for analysis of the iron sulfur cluster content in an anaerobic MBraun Box (<1 ppm O_2). Oxidized samples were prepared by addition of 5 mM potassium ferricyanide and were incubated for 20 minutes before flash freezing. Photo reduced samples were prepared by supplementing the protein with 50 mM Tris pH 7.4, 100 μM deazariboflavin, and 5 mM dithiothreitol (DTT). Samples were then placed in an ice water bath and illuminated with a 300 watt Xe light for one hour. To an additional photo reduced sample, 2 mM GTP was added to both H306Q and C353S HydF^{ΔEG} in the

absence of light and both samples were flash frozen in liquid nitrogen. Samples were stored in liquid nitrogen until spectroscopic analysis.

Low temperature EPR analysis was performed using a Bruker EMX X-band spectrometer equipped with a liquid helium cryostat and Oxford Instrument temperature controller. Typical EPR parameters were: 9.37 GHz microwave frequency, 1.84 mW microwave power, 12 K sample temperature, 81.92 ms time constant, and 167.7 s time sweep. EPR data simulation was performed using the EasySpin software program. To study the temperature dependence of the iron sulfur cluster content, the EPR spectrum of the H306Q and C353S photo reduced sample was studied from 12 K up to 60 K in 10 K increments.

In vitro Hydrogenase Activity Assays

The ability of the substituted HydF^{EG} proteins to activate HydA^{ΔEFG} as compared to WT HydF^{EG} was tested. The assay involved combining purified inactive HydA^{ΔEFG} with the respective purified HydF^{EG} substituted protein, in addition to methyl viologen and dithionite (45). In this assay, dithionite serves as an electron donor with methyl viologen acting as an electron conduit to HydA. Assay mixtures were prepared in a Coy anaerobic chamber at 25°C by mixing HydA^{ΔEFG} (1.47μM) with an excess of purified maturation protein (~14.7μM) in 3 ml sealable glass vials. Every 2 ml reaction was performed in buffer (50 mM HEPES, pH 7.5, 100 mM KCl) in the presence of 20 mM sodium dithionite. The reactions were sealed, removed from the anaerobic chamber, and degassed to remove residual hydrogen from the headspace. Hydrogenase assays were performed at 25°C and initiated by the addition of oxidized ethyl viologen (10 mM final

concentration) and the production of H₂ was monitored using gas chromatography as described previously (45).

DATA AND RESULTS

The primary aim of the aforementioned experiments was to identify the ligands for both [4Fe-4S] and [2Fe-2S] clusters in HydF. In order to achieve this objective each of the variants of HydF containing the amino acid substitutions was isolated from *C. acetobutylicum* and each substituted HydF is expressed with or without HydE, HydG. In all cases the purified substituted protein was characterized and analyzed further by UV-Vis spectroscopy and EPR analysis. The purified aforementioned proteins exhibited shades of brown color as compared to the wild type (WT) HydF^{ΔEG} indicating presence of the iron sulfur species. The variant HydF^{ΔEG} C304S, C304A and C356A were colorless, while H306Q, H306N, H306A, C353S, C353A, C356S had different shades of brown depending on the Fe-S content.

Iron Content of Substituted HydF^{ΔEG} Proteins

The iron content of wild type (WT) and substituted HydF^{ΔEG} proteins were quantified to gain an insight into the effect of amino acid substitutions on iron-sulfur cluster assembly. The low iron contents of the C304 and C356 variants suggested that these two residues are crucial for iron sulfur cluster assembly and their substitution reduces the overall iron loading (Table.2).

Histidine306 substitution to glutamine or asparagine have iron numbers comparable to that of the WT while H306 substitution to alanine was shown to have lower iron number indicating an inefficient Fe-S cluster assembly. The C353S protein is comparable with that of the WT but the C353A protein showed a significant decrease in

iron content, although not as drastic as C304A and C356A substitutions. Therefore in order to gain more insights into ability of these substituted HydF^{ΔEG} to form the Fe-S cluster, we performed UV-Vis Spectroscopic studies of WT and substituted HydF^{ΔEG}.

Table 2: Iron assay for WT and substituted HydF^{ΔEG}.

Protein	Fe atoms per mole of protein
HydF ^{ΔEG}	1.23 ±0.03
HydF ^{ΔEG} C304S	0.10±0.05
HydF ^{ΔEG} C304A	0.14±0.04
HydF ^{ΔEG} H306Q	1.57±0.05
HydF ^{ΔEG} H306N	1.00±0.02
HydF ^{ΔEG} H306A	0.34±0.03
HydF ^{ΔEG} C353S	1.23±0.03
HydF ^{ΔEG} C353A	0.7±0.01
HydF ^{ΔEG} C356S	0.50±0.09
HydF ^{ΔEG} C356A	0.03±0.03

Uv-Vis Absorption Spectroscopy of Substituted HydF^{ΔEG} Proteins

Uv-vis spectroscopy is used to identify presence of Fe-S clusters. We compared the absorption spectra of WT and substituted HydF^{ΔEG}. The spectral features of Fe-S clusters can be observed in the visible range (300-800nm). These absorption bands are derived from the S to Fe charge transfer. The WT HydF^{ΔEG} show spectral features at ~350nm, ~420nm, ~510nm and ~ 600nm which are suggestive of Fe-S clusters. The absorption spectra of the C304S and C304A proteins (Fig.8a), though largely featureless,

showed a low signal intensity feature ~ 410 nm. This indicated small amount of Fe-S cluster assembly in both C304S/A. This is consistent with the low iron numbers reported for these altered proteins in Table.1 and strongly suggests that the cysteine residue at position 304 affects the iron sulfur cluster assembly drastically.

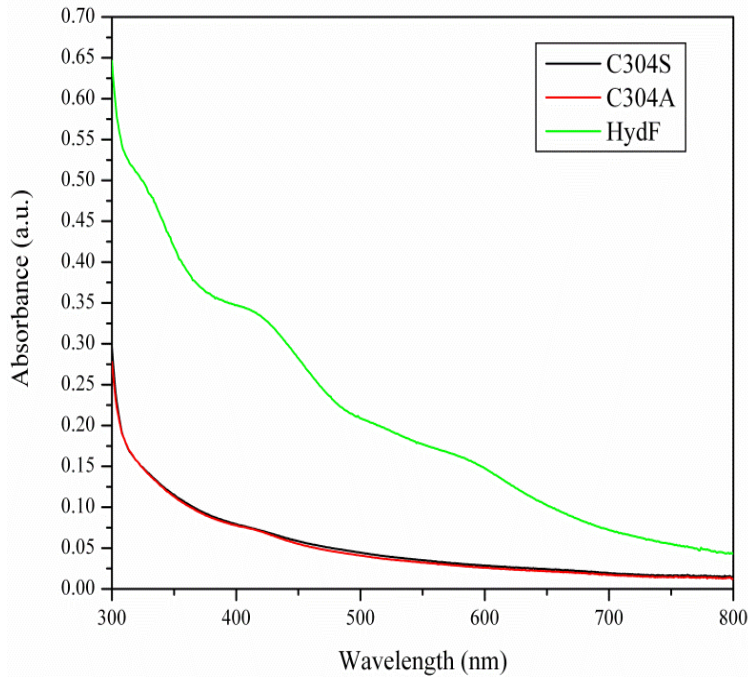


Fig.8a: UV-Vis absorption spectra of WT, C304S and C304A HydF^{ΔEG} *C. acetobutylicum* (50 μ M each). The optical pathlength was 1cm.

The trend for spectral features of the histidine306 substituted residues (Fig.8b) appeared to be different than cysteine304. The H306Q HydF^{ΔEG} shows a slight increase in the signal intensity at ~ 410 nm and at ~ 570 nm region as compared to the WT spectrum. However the iron numbers for this mutant were comparable with WT, thereby indicating that H306Q had similar Fe-S cluster content as the WT.

The spectrum of H306N appeared to have a similar spectrum but with low signal intensity to that of the WT and the Fe numbers between the two was also not drastically different.

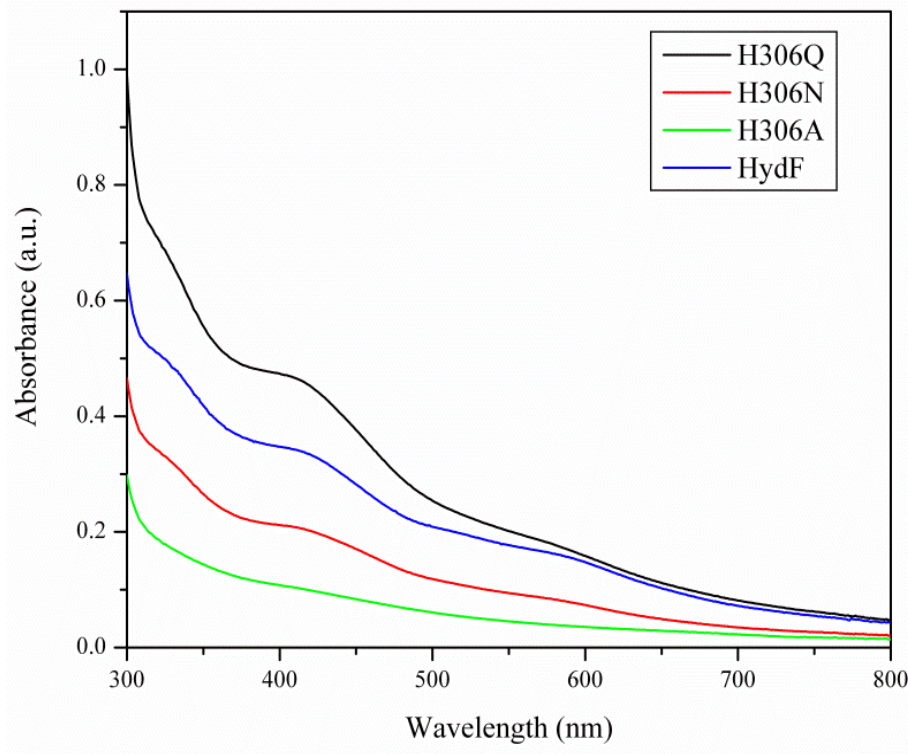


Fig.8b: UV-Vis Absorption spectra of WT, H306Q, H306N and H306A HydF^{ΔEG} *C. acetobutylicum* (50 μ M protein each). The optical pathlength was 1cm.

This data suggested that a similar type of cluster/s were bound to H306N as the WT (Fig.8b). The H306A substituted protein appeared to exhibit reduced spectral intensities around 400-600nm which agreed well with the significantly low iron numbers of this altered protein as compared to the WT protein (Fig.8b). This result indicates that the change in chemical coordination has a considerable affect on both [2Fe2S] and [4Fe4S] types of iron sulfur clusters.

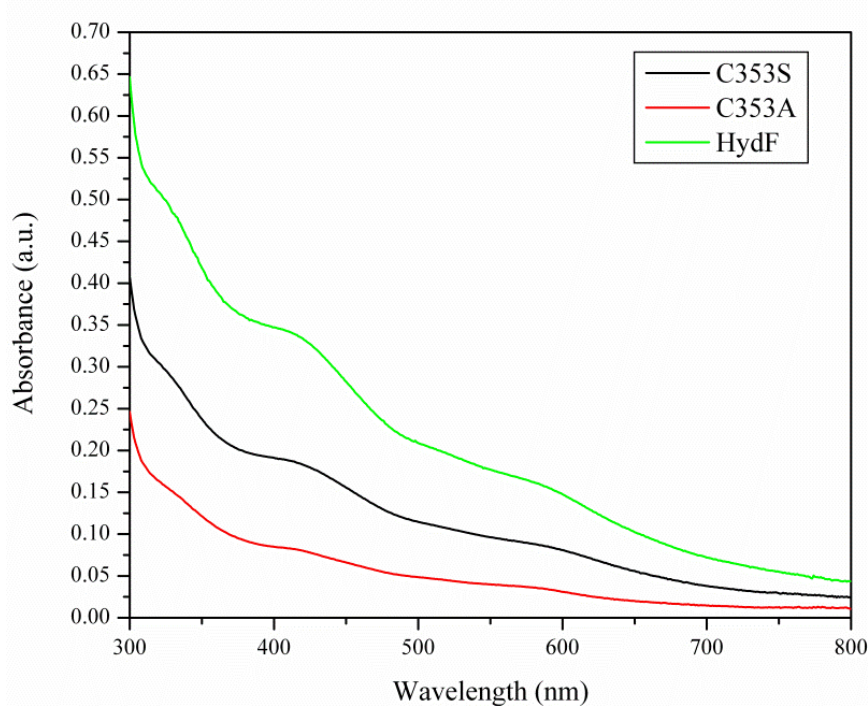


Fig.8c: UV-Vis Absorption spectra of WT, C353S and C353A HydF^{ΔEG} *C. acetobutylicum* (50 μM each). The optical pathlength was 1cm.

The spectra obtained from C353S and C353A (Fig.8c) exhibited a slight shift of ~6nm in the 400-450 nm region and a ~4 nm shift in 500-600 nm region as compared to the WT. The decreased absorbance observed for C353A substitution was in agreement with its low iron number. However the iron numbers observed for the C353S mutant were similar to that of the WT HydFHydF^{ΔEG} but the spectral intensities were almost half as that of the WT. This suggested that the Fe-S cluster assembly in C353S is not similar as that of the WT. The similar iron number of C353S and the WT may indicate the presence of exogenously bound iron in C353S.

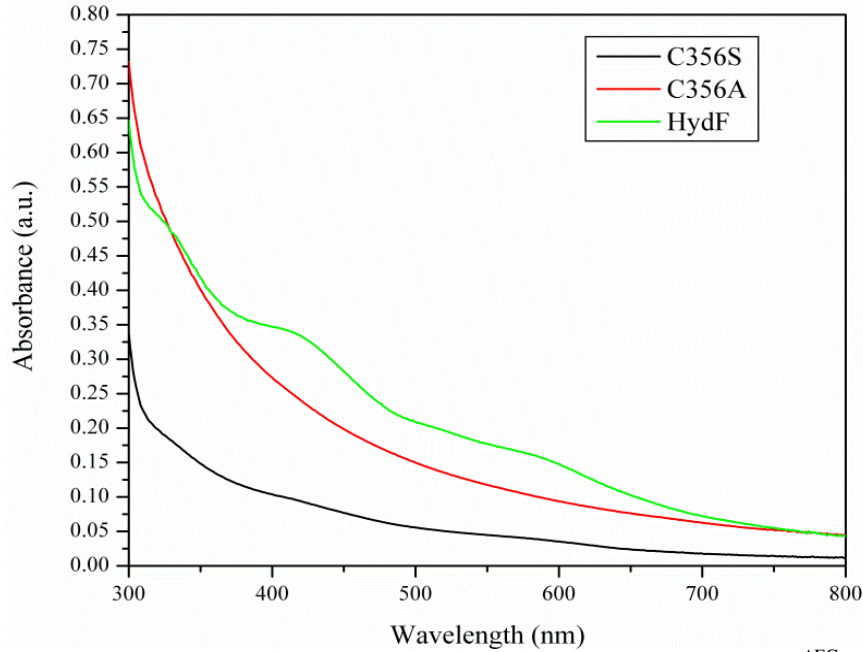


Fig.8d: UV-Vis absorption spectra of WT, C356S and C356A HydF^{ΔEG} *C. acetobutylicum* (50 μM each). The optical pathlength was 1cm.

The C356S appeared to have a similar spectral feature as the WT protein albeit with significantly reduced intensities (Fig.8d). This was again in agreement with the lower iron numbers associated with this substitution (Table.2).

The C356A substituted HydF^{ΔEG} was shown to have extremely low iron levels which were further indicated by a completely featureless UV-Vis spectrum (Fig.8d) (Table.2).

EPR Spectroscopy

C353S HydF^{ΔEG}

The EPR spectrum of the as isolated C353S HydF^{ΔEG} (Fig.9a) displayed very low signal intensity spectrum but had similar g values to that of the oxidized HydF^{EG} (Unpublished results by Shepard et al). This signal however was not detected when the

C353S substituted protein was photo-reduced (Fig.9b) and spectral features suggestive of a $[4\text{Fe-4S}]^+$ cluster were observed. This $[4\text{Fe-4S}]^+$ cluster had different g values than the as-isolated C353S form but were identical to that of the reduced WT $\text{HydF}^{\Delta\text{EG}}$ form. Addition of GTP in the photo-reduced sample neither enhanced the signal intensity nor shifted the apparent g value, changes which were distinctive features observed in the case of WT $\text{HydF}^{\Delta\text{EG}}$ (30). These results suggested that C353S $\text{HydF}^{\Delta\text{EG}}$ binds similar $[4\text{Fe-4S}]^+$ cluster as the WT.

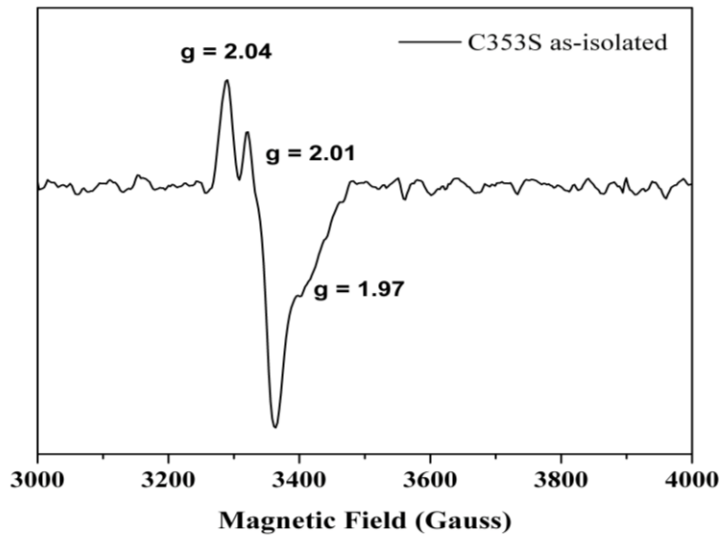


Fig.9a: Low temperature EPR signal of as-isolated C353S $\text{HydF}^{\Delta\text{EG}}$ ($g = 2.04, 2.01, 1.97$)

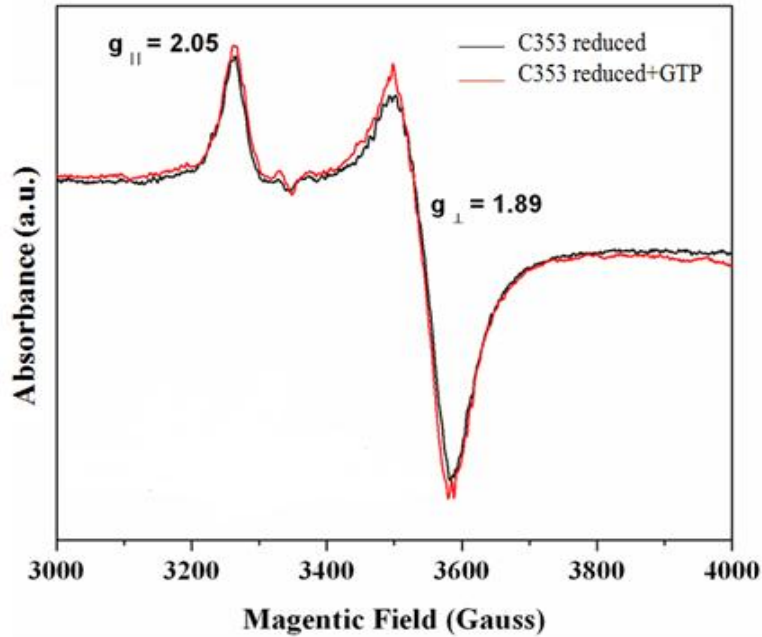


Fig.9b: Low temperature EPR signal of reduced C353S HydF^{ΔEG} shows presence of a [4Fe4S]⁺ ($g_{\perp} = 1.89$ and $g_{\parallel} = 2.05$). C353S HydF^{ΔEG}-Black line- w/o GTP, Red line- with GTP

H306Q HydF^{ΔEG}

The as-isolated H306Q HydF^{ΔEG} sample exhibited an EPR signal with g-values at 2.00 and 1.96, suggestive of some [2Fe-2S]⁺ content, overlaid on a signal with g-values at 2.05 and 1.90 that are very similar to the [4Fe-4S]⁺ cluster observed in reduced WT HydF^{ΔEG} (Fig.10a). To further confirm presence of two different types of Fe-S clusters we performed a temperature dependence EPR on as-isolated H306Q sample like it was done previously on WT. It was observed that by 30K one type of cluster signal had completely disappeared while the second type of cluster signal was present up to 50K. This rapid signal loss with increasing temperature is characteristic of a [4Fe-4S]⁺ cluster while the remaining signal at 50 K is suggestive of a [2Fe-2S]⁺ cluster with a signal relaxation that is much less dependent on temperature (Fig.10c.).

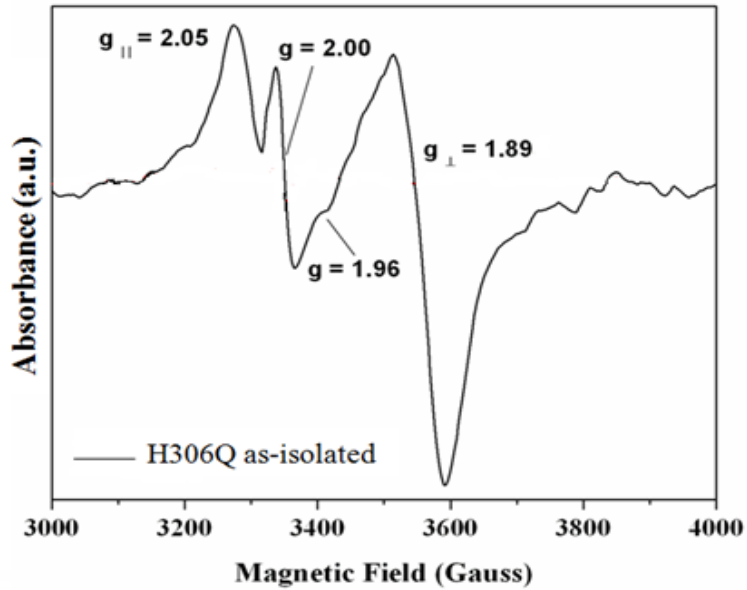


Fig.10a: Low temperature EPR signal of as-isolated H306Q HydF^{ΔEG} shows presence of a [4Fe-4S]⁺ ($g_{\perp} = 1.895$ and $g_{\parallel} = 2.05$) and [2Fe-2S]⁺ cluster ($g = 2.00, 1.96$).

This result seems to be relevant with the UV-Vis spectroscopic and metal content observations.

Interestingly the photo reduced H306Q HydF^{ΔEG} displayed a single signal indicative of a [4Fe-4S]⁺ cluster with similar g values to the reduced WT HydF^{ΔEG} protein. The lack of any significant g -value shift may suggest that the electronic state of the [4Fe-4S]⁺ cluster is very similar to that observed in the WT protein.

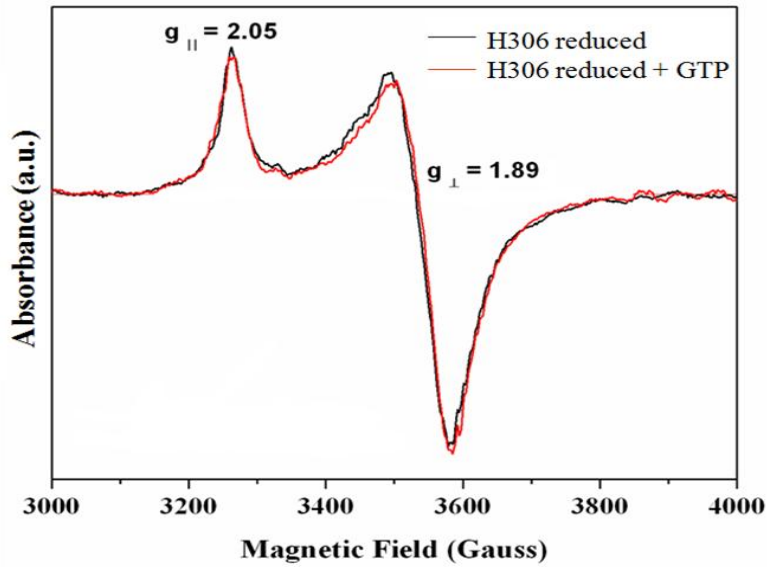


Fig.10b: Low temperature EPR signal of reduced H306Q HydF^{AEG} shows presence of a [4Fe4S]⁺ ($g_{\perp} = 1.89$ and $g_{\parallel} = 2.05$). H306Q HydF^{EG}- Black line- w/o GTP, Red line- with GTP

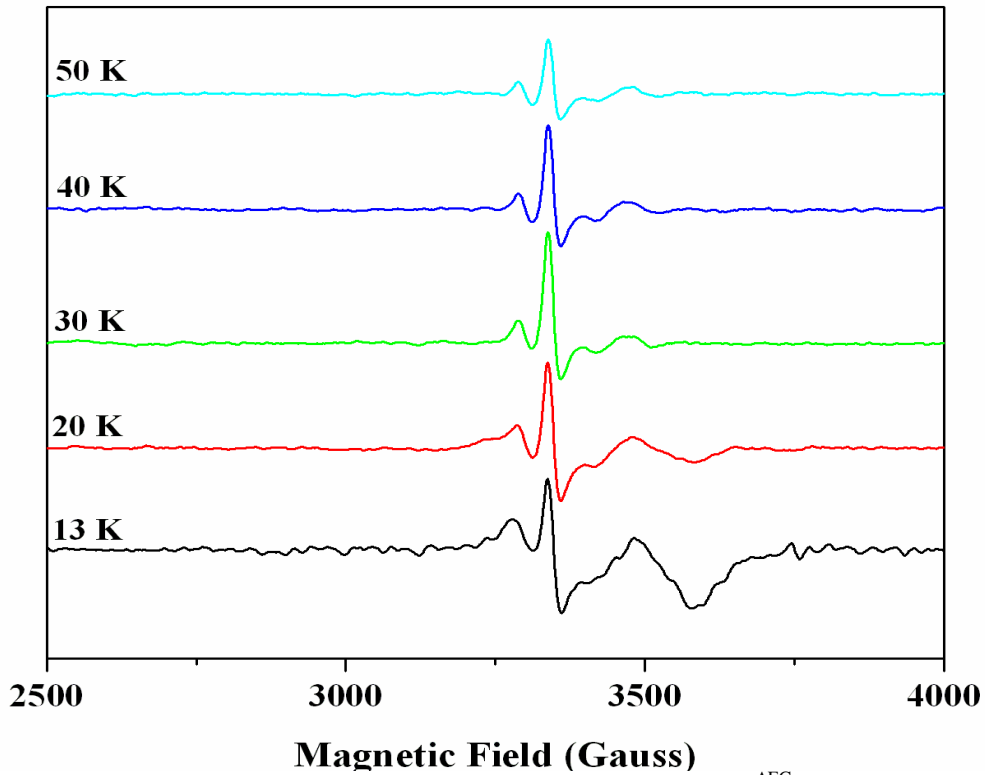


Fig.10c: Temperature dependence of as-isolated sample of HydF^{AEG} H306Q in the presence of MgCl₂ (5 mM). EPR parameters are given in experimental procedures. Both samples were run at a constant power setting (1.85 mW) at the temperature values given for each spectrum.

Upon addition of GTP to reduced H306Q HydF^{ΔEG}, no perturbation in the [4Fe-4S]⁺ cluster signal intensity is obtained, similar to what was observed with the C353S reduced plus GTP sample.

In vitro Hydrogenase Activity Assays

In order to investigate if the mutation of conserved amino acid residues in the iron sulfur cluster binding region plays any role in the transfer of the H-cluster precursor to generate active hydrogenase, we decided to perform hydrogenase activation assays. We have shown before that WT HydF^{EG} acts as a surrogate on which the assembly of the precursor happens, which after completion gets delivered to HydA (28, 30). Thus we performed similar experiment to understand the importance of these conserved residues in the maturation of HydA. We purified substituted and WT HydF in the background of HydE and HydG. Further we incubated each of the HydF^{EG} substituted and WT proteins with inactive purified HydA^{ΔEFG} at room temperature and further assayed them for hydrogenase activity as explained before. The hydrogenase activity results are displayed in (Fig.11), suggesting that besides WT HydF^{EG}, the mutants HydF^{EG} H306Q and HydF^{EG} H306A have the ability to activate HydA^{ΔEFG}. However the competence of the H306Q mutant and H306A mutant to activate HydA^{ΔEFG} is ~10 fold and ~30 fold less than that of the WT HydF^{EG}. None of the other HydF^{EG} mutants have the ability to activate hydrogenase to any measureable extent.

These results indicate the essential role of C304, C353 and C356 residues in either assembly and/or transfer of the precursor for H-cluster activation.

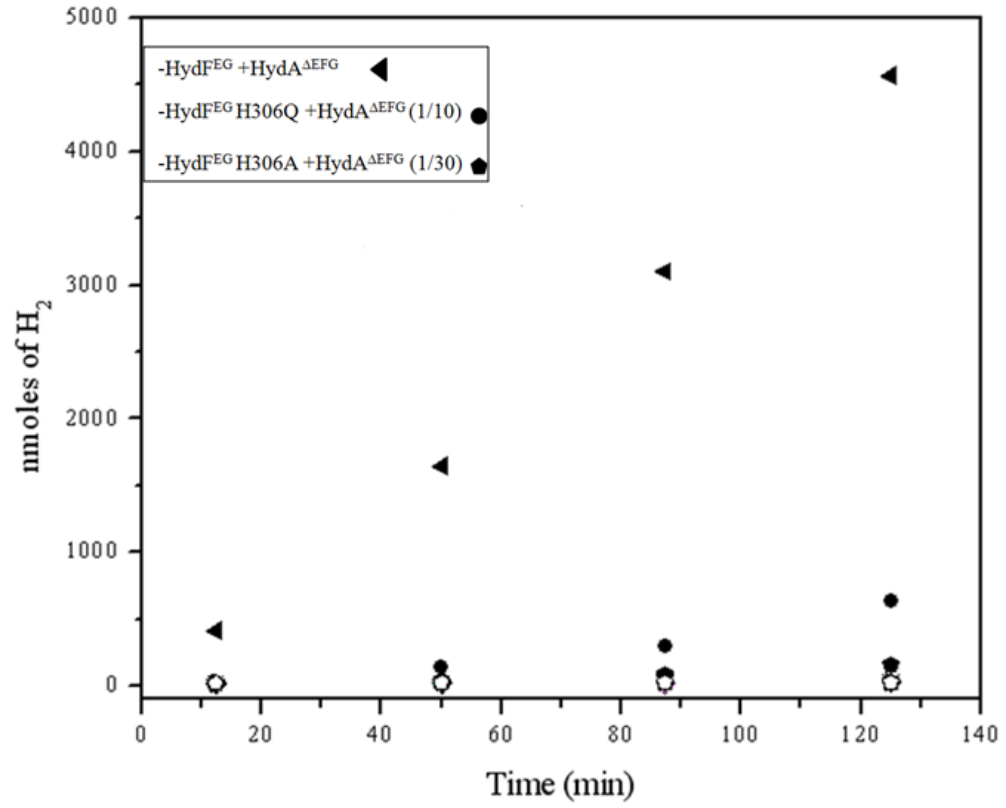


Fig. 11: H₂ evolution assays to probe the effects of HydF mutations on the activation of HydA^{ΔEFG} by HydF^{EG}.

DISCUSSION

The biosynthetic pathway for the H-cluster of [FeFe]-hydrogenase requires 3 Hyd accessory proteins namely HydE, HydG and HydF (18). HydF is a GTPase and contains a [2Fe-2S] and [4Fe-4S] clusters supposedly bound by putative CxH_{x45-53}CxxC conserved residues (20, 22, 30). It is unclear that how each type of cluster most importantly the 2Fe species is bound in HydF. Thus we substituted each putative Fe-S cluster binding residue and analyzed the changes in individual clusters by spectroscopic methods as well as biochemical assays.

Our initial iron assays and UV-Vis spectroscopic analysis of the altered HydF^{ΔEG}s and WT HydF^{ΔEG} suggested that the substitutions at either C304 or C356 are detrimental for any type of iron sulfur cluster assembly however the substitutions in H306 and C353 are not absolutely essential for Fe-S cluster assembly.

Previously it had been shown that reduced HydF^{ΔEG} exhibited an EPR spectrum characteristic of [4Fe-4S]⁺ and [2Fe-2S]⁺ clusters and the signal intensities of both clusters increased in the presence of GTP. These results implicated the possibility of “cross talk” between the GTP binding domain and Fe-S cluster binding domain in HydF (30). Our EPR spectroscopic studies of the reduced H306Q and reduced C353S HydF^{ΔEG} have confirmed that these substituted proteins have a similar [4Fe-4S]⁺ cluster as that of the reduced WT HydF^{ΔEG}; however we have observed that the signal for the [2Fe-2S]⁺ cluster is considerably affected in both these cases. Also, no perturbations in EPR signal intensity were observed after GTP addition in either of the altered proteins suggesting that the above substitutions may have interrupted the communication between the GTP

binding domain and the Fe-S cluster binding domain. One possible explanation for this could be that both the H306Q and C353S HydF^{ΔEG} have an altered protein conformation which disrupted the interplay between GTP binding and cluster binding sites and only additional studies will clarify this issue.

It was confirmed from our previous results that HydE and HydG are required for transformation of the [2Fe-2S] cluster on HydF to a 2Fe subcluster which is then delivered to HydA^{ΔEFG}. Thus we performed *in vitro* hydrogenase activity assays to assess the ability of the substituted HydF^{EG} to activate HydA^{ΔEFG}. The results from the *in vitro* hydrogenase activity assays suggests that only H306 substituted HydF^{EG} had some capacity to activate [FeFe]-hydrogenase but only at significantly reduced rates relative to WT hydF^{EG}. These results indicated that residue H306 is critical in either assembly or transition of fully accessorized 2Fe species to HydA^{ΔEFG}. On the contrary, we observed that the C353 substitutions were completely unable to activate HydA^{ΔEFG}. This suggests that cysteine 353 is involved in proper 2Fe subcluster formation in HydF.

Thus we combined our present observations with the previous structural, spectroscopic and oligomeric analysis of WT HydF to design two possible scenarios for the assignment of ligands for both for both the [2Fe-2S] cluster and the [4Fe-4S] cluster. The dimeric/ tetrameric (dimer of dimers) nature of HydF brings four residues together at domain interface, thus providing eight putative ligands for cluster binding. The perturbations in residues cysteine 304 and 356 resulted in no Fe-S cluster assembly, thus it is possible that cysteine 304 and 356 are critical for dimer interface formation and may bind the [4Fe-4S] cluster. The available data suggests that the [4Fe-4S] cluster more

readily forms and perturbations in its ligand environment may preclude [2Fe-2S] cluster binding. Thus substitutions at C304 and C356 appear to abolish both the [4Fe-4S] and the [2Fe-2S] cluster binding. The results with cysteine 353 substitutions suggest that this ligand coordinates the [2Fe-2S] cluster. Furthermore, previous HYSCORE observations suggested that the hyperfine coupling constant values of reconstituted HydF^{ΔEG} from *T. maritima* are in the range of those obtained for [2Fe-2S] cluster Rieske proteins (22). Since the 2Fe subcluster assembly and/or transfer get affected by the H306 substitutions, we propose that it could be the other residue which binds the [2Fe-2S] cluster (Fig.12A).

Another possible scenario for Fe-S cluster ligation environment is shown in (Fig.12B). This example highlights the possibility that the conserved histidine 306 coordinates the [4Fe-4S] cluster which was supported by pulsed EPR ¹⁴N measurements of the [4Fe-4S] cluster in HydF^{EG} from *C. acetobutylicum* (41). The H306N and H306A substitutions clearly affects the Fe-S cluster assembly in HydF^{ΔEG} and all H306 substituted HydF^{EG} show significantly retarded HydA^{ΔEFG} activation rates, thus supporting the ligation of this histidine 306 residue to Fe-S cluster.

Further advanced spectroscopic studies and crystal structure of holo HydF would shed more light on the exact coordination of the Fe-S clusters. If the proposed model in (Fig.12B) proves to be true then that would add up on the growing evidence for non cysteinyl coordination in the iron sulfur clusters.

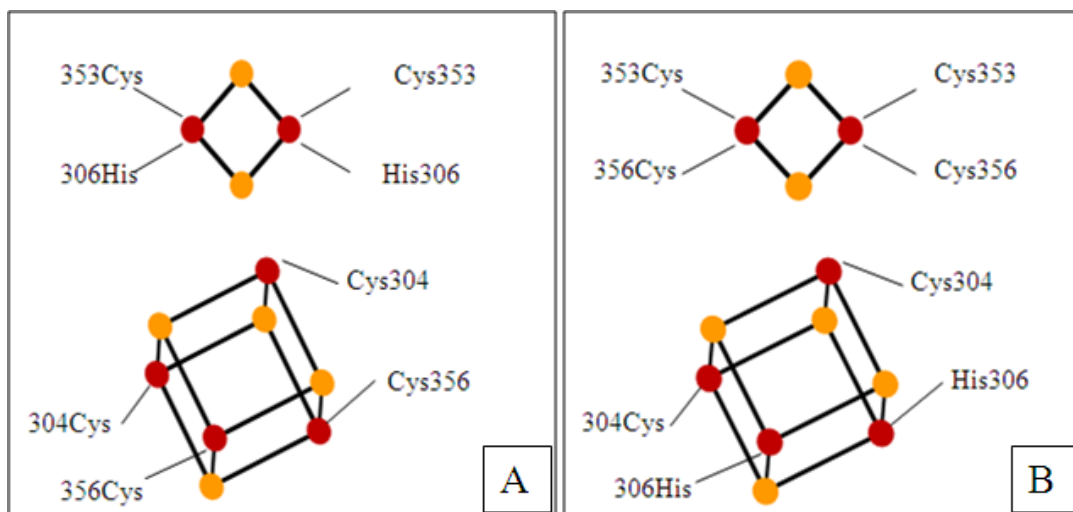


Fig. 12: Proposed models (A and B) for putative ligations of the [4Fe-4S] and the [2Fe-2S] clusters to the HydF polypeptide chain as inferred from the site directed mutagenesis experiments.

REFERENCES

1. Beinert, H., Holm, R. H., and Munck, E. (1997) *Iron-sulfur clusters: nature's modular, multipurpose structures. Science* 277, 653-9.
2. Beinert, H., and Kiley, P. J. (1999) *Fe-S proteins in sensing and regulatory functions. Curr Opin Chem Biol* 3, 152-7.
3. Lennarz, W. J., Lane, M. D., and ScienceDirect (Online service). (2004), Elsevier, Amsterdam; Boston.
4. Capozzi, F., Ciurli, S., and Luchinat, C. (1998) *Coordination sphere versus protein environment as determinants of electronic and functional properties of iron-sulfur proteins. Metal Sites in Proteins and Models* 90, 127-160.
5. Berkovitch, F., Nicolet, Y., Wan, J. T., Jarrett, J. T., and Drennan, C. L. (2004) *Crystal structure of biotin synthase, an S-adenosylmethionine-dependent radical enzyme. Science* 303, 76-79.
6. Cammack, R. (1999) *Hydrogenase sophistication. Nature* 397, 214-215.
7. Adams, M. W. (1990) *The structure and mechanism of iron-hydrogenases. Biochim Biophys Acta* 1020, 115-145.
8. Przybyla, A. E., Robbins, J., Menon, N., and Peck, H. D., Jr. (1992) *Structure-function relationships among the nickel-containing hydrogenases. FEMS Microbiol Rev* 8, 109-135.
9. Adams, M. W., and Stiefel, E. I. (1998) *Biological hydrogen production: not so elementary. Science* 282, 1842-1843.
10. Adams, M. W., Mortenson, L. E., and Chen, J. S. (1980) *Hydrogenase. Biochim Biophys Acta* 594, 105-176
11. Vignais, P. M., and Billoud, B. (2007) *Occurrence, classification, and biological function of hydrogenases: an overview. Chem Rev* 107, 4206-72.
12. Volbeda, A., Cheron, M.H., Piras, C., Hatchikian, E. C., Frey, M., and Fontecilla-Camps, J.C., (1995) *Crystal structure of the nickel-iron hydrogenase from Desulfovibrio gigas Nature*, 1995,375, 580-587
13. Peters, J. W., Lanzilotta, W. N., Lemon, B. J., and Seefeldt, L. C. (1998) *X-ray crystal structure of the Fe-only hydrogenase (CpI) from Clostridium pasteurianum to 1.8 angstrom resolution. Science* 282, 1853-1858.

14. Nicolet, Y., Piras, C., Legrand, P., Hatchikian, C. E., and Fontecilla-Camps, J. C. (1999) *Desulfovibrio desulfuricans* iron hydrogenase: the structure shows unusual coordination to an active site Fe binuclear center. *Structure Fold Des* 7, 13-23.
15. Nicolet, Y., de Lacey, A. L., Vernede, X., Fernandez, V. M., Hatchikian, E. C., and Fontecilla-Camps, J. C. (2001) Crystallographic and FTIR spectroscopic evidence of changes in Fe coordination upon reduction of the active site of the Fe-only hydrogenase from *Desulfovibrio desulfuricans*. *J Am Chem Soc* 123, 1596-1601.
16. Nicolet, Y., Lemon, B. J., Fontecilla-Camps, J. C., and Peters, J. W. (2000) A novel FeS cluster in Fe-only hydrogenases. *Trends Biochem Sci* 25, 138-143.
17. Silakov A, Wenk B, Reijerse E, Lubitz W. (14) N HYSCORE investigation of the H-cluster of [FeFe] hydrogenase: evidence for a nitrogen in the dithiol bridge. *Phys Chem Chem Phys*. 2009 Aug 21;11(31):6592-9. Epub 2009 Jun 9.
18. Posewitz, M. C., King, P. W., Smolinski, S. L., Zhang, L., Seibert, M., and Ghirardi, M. L. (2004) Discovery of two novel radical S-adenosylmethionine proteins required for the assembly of an active [Fe] hydrogenase. *J Biol Chem* 279, 25711-20.
19. Frey, P. A. (2001) Radical mechanisms of enzymatic catalysis. *Annu Rev Biochem* 70, 121-48.
20. King, P., W., Posewitz, M. C., Ghirardi, M. L. Seibert, M. (2006) Functional Studies of [FeFe] Hydrogenase Maturation in an *Escherichia coli* Biosynthetic System. *J Bact*,(2006)2163-2172
21. McGlynn, S. E., Ruebush, S. S., Naumov, A., Nagy, L. E., Dubini, A., King, P. W., Broderick, J. B., Posewitz, M. C., and Peters, J. W. (2007) In vitro activation of [FeFe] hydrogenase: new insights into hydrogenase maturation. *J Biol Inorg Chem* 12, 443-7.
22. Brazzolotto, X., Rubach, J. K., Gaillard, J., Gambarelli, S., Atta, M., and Fontecave, M. (2006) The [Fe-Fe]-hydrogenase maturation protein HydF from *Thermotoga maritima* is a GTPase with an iron-sulfur cluster. *Journal of Biological Chemistry* 281, 769-774.
23. Rubach, J.K., Brazzolotto, X., Gaillard, J. and Fontecave, M. (2005) Biochemical characterization of the HydE and HydG iron-only hydrogenase maturation enzymes from *Thermotoga maritima*. *FEBS Lett.* 579, 5055–5060.
24. Ugulava, N. B., Gibney, B. R., and Jarrett, J. T. (2001) Biotin synthase contains two distinct iron-sulfur cluster binding sites: Chemical and spectroelectrochemical analysis of iron-sulfur cluster interconversions. *Biochemistry* 40, 8343-8351.

25. Kriek, M., Martins, F., Challand, M.R., Croft, A. and Roach, P.L. (2007) Thiamine biosynthesis in *Escherichia coli*: identification of the intermediate and byproduct derived from tyrosine. *Angew. Chem. Int. Ed.* 46, 9223–9226
26. Nicolet, Y., Rubach, J.K., Posewitz, M.C., Amara, P., Mathevon, C., Atta, M., Fontecave, M., and Fontecilla-Camps, J.C. (2008) X-ray Structure of the [FeFe]-Hydrogenase Maturase HydE from *Thermotoga maritime*. *Journal of Biological Chemistry* VOL. 283, NO. 27, pp. 18861–18872
27. Peters, J. W., Szilagy, R. K., Naumov, A., and Douglas, T. (2006) A radical solution for the biosynthesis of the H-cluster of hydrogenase. *FEBS Lett* 580, 363-7.
28. McGlynn, S. E., Shepard, E., M., Winslow, M.A., Naumov, A., Nagy, Duschene K.S., Posewitz M.C., W., Broderick, J. B., Posewitz, M. C., and Peters, J. W. (2008) HydF as a scaffold protein in [FeFe]hydrogenase H-cluster biosynthesis. *FEBS Letters* 582 (2008) 2183–2187
29. Pilet, E., Nicolet, Y., Mathevon, C., Douki, T., Fontecilla-Camps, J.C., Fontecave, M. (2009) The role of maturase HydG in [FeFe]-hydrogenase active site synthesis and assembly. *FEBS Letters* 583(2009) 506-511
30. Shepard EM, McGlynn SE, Bueling AL, Grady-Smith CS, George SJ, Winslow MA, Cramer SP, Peters JW, Broderick JB. Synthesis of the 2Fe subcluster of the [FeFe]-hydrogenase H cluster on the HydF scaffold, *Proc Natl Acad Sci U S A.* 2010 Jun 8;107(23):10448-53.
31. Bradford, M. M. (1976) A Rapid and Sensitive Method for the Quantitation of Microgram Quantities of Protein Utilizing the Principle of Protein-Dye Binding. *Anal. Biochem.* 72:248-254
32. Mulder, D.,W., Ortillo, D.,O., Gardenghi, D., J., Naumov, Anatoli., V., Ruebush, S., S., Szilagy, R., K., Huynh, B., Broderick, J., B., Peters, J., W. (2009) Activation of HydA^{ΔEFG} Requires a Preformed [4Fe-4S] Cluster *Biochemistry*, 2009, 48 (26), pp 6240–6248
33. Sofia, H. J.; Chen, G.; Hetzler, B. G.; Reyes-Spindola, J. F.; Miller, N. E.. Radical SAM, a novel protein superfamily linking unresolved steps in familiar biosynthetic pathways with radical mechanisms: functional characterization using new analysis and information visualization methods. *Nucleic Acids Research*, 2001, 29, 1097-1106.
34. Jarrett, J.T.. The generation of 5'-deoxyadenosyl radicals by denosylmethioninedependent radical enzymes. *Curr. Opin. Chem. Biol.*, 2003, 7, 174-182

35. Driesener RC, Challand MR, McGlynn SE, Shepard EM, Boyd ES, Broderick JB, Peters JW, Roach PL. [FeFe]-hydrogenase cyanide ligands derived from S-adenosylmethionine-dependent cleavage of tyrosine. *Angew Chem Int Ed Engl.* 2010 Feb 22;49(9):1687-90.
36. Shepard EM, Duffus BR, George SJ, McGlynn SE, Challand MR, Swanson KD, Roach PL, Cramer SP, Peters JW, Broderick JB. [FeFe]-hydrogenase maturation: HydG-catalyzed synthesis of carbon monoxide. *J Am Chem Soc.* 2010 Jul 14; 132(27):9247-9.
37. Fish, M. W. (1988) *Methods Enzymol* 158, 357-364
38. Scrima, A., Vetter, I.R., Armengod, M.E., Wittinghofer, A. (2005) The structure of the TrmE GTP-binding protein and its implications for tRNA modification(2005) *Embo J.* 24: 23-33
39. Rangaraj, P.; Tyle, M. J.; Lanzilotta, W. N.; Ludden, P. W.; Shah, V. K.. In Vitro Biosynthesis of Iron-Molybdenum Cofactor and Maturation of the nef-encoded Apodinitrogenase. *J. Biol. Chem.*, 1999, 274, 19778-19784
40. Waldron, K. J.; Robinson, N. J. How do bacterial cells ensure that metalloproteins get the correct metal?. *Nat. Rev. Microbi.*, 2009, 6, 25-35.
41. Czech I, Silakov A, Lubitz W, Happe T. The [FeFe]-hydrogenase maturase HydF from *Clostridium acetobutylicum* contains a CO and CN- ligated iron cofactor. *FEBS Lett.* 2010 Feb 5;584(3):638-42
42. Czech I, Stripp S, Sanganas O, Leidel N, Happe T, Haumann M. The [FeFe]-hydrogenase maturation protein HydF contains a H-cluster like [4Fe4S]-2Fe site. *FEBS Lett.* 2011 Jan 3; 585(1):225-30.
43. Mulder DW, Boyd ES, Sarma R, Lange RK, Endrizzi JA, Broderick JB, Peters JW. Stepwise [FeFe]-hydrogenase H-cluster assembly revealed in the structure of HydA(DeltaEFG). *Nature.* 2010 May 13;465(7295):248-51
44. Mulder DW, Shepard EM, Meuser JE, Joshi N, King PW, Posewitz MC, Broderick JB, Peters JW; Insights into [FeFe]-hydrogenase structure, mechanism, and maturation. *Structure.* 2011 Aug 10;19(8):1038-52
45. Peck HD, Gest H. A new procedure for assay of bacterial hydrogenases. *J Bacteriol* 1956, 71:70-80
46. Meyer J., Fujinaga J., Gaillard J., Lutz ; Mutated Forms of the [2Fe-2S] Ferredoxin from *Clostridium pasteurianum* with Noncysteinyl Ligands to the Iron-Sulfur Cluster. *Biochemistry*, 1994, 33 (46), pp 13642-13650.

47. Martín AE, Burgess BK, Stout CD, Cash VL, Dean DR, Jensen GM, Stephens PJ; Site-directed mutagenesis of *Azotobacter vinelandii* ferredoxin I: [Fe-S] cluster-driven proteinrearrangement. *Proc Natl Acad Sci U S A*. 1990 Jan; 87(2):598-602.
48. Cendron L, Berto P, D'Adamo S, Vallese F, Govoni C, Posewitz MC, Giacometti GM, Costantini P, Zanutti G; Crystal structure of HydF_scaffold protein provides insights into [FeFe]-hydrogenase maturation. *J Biol Chem*. 2011 Dec 23;286(51):43944-50
49. Nicolet Y, Fontecilla-Camps JC; Structure-Function Relationships in [FeFe]-Hydrogenase Active Site Maturation. *J Biol Chem*. 2012 Mar 2